

Double -Diffusive Magnetohydrodynamic flow of Williamson Nanofluid past a horizontally positioned stretching cylinder in a porous medium with effect of thermophoresis and Brownian motion

Adekanmbi- Akinseye Adejoke¹, Fenuga Olugbenga²

¹Department of Mathematics, faculty of science, University of Lagos, Nigeria

²: Department of Mathematics, University of Lagos, Nigeria

ABSTRACT

The goal of this study is to determine the flow pattern and behavior of a steady two-dimensional, double diffusive MHD flow of Williamson nanofluid past a permeable horizontally placed stretching cylinder in a porous medium. The modelled partial differential equations are converted into coupled, non linear ordinary differential equations through similarity variable transformations. The Homotopy Perturbation Method (HPM) is used to solve analytically the resulting system of linked, nonlinear ordinary differential equations. HPM is a methodical approach that ignores the linearization and discretization processes to produce precise analytical solutions of nonlinear equations. The numerical scheme of the fourth order Runge-Kutta integration using shot technique and the results of the Homotopy perturbation method (HPM) are compared, and the findings show great agreement with the literature. While the impact of relevant flow parameters on physical engineering of interest, such as the skin friction coefficient, Nusselt number and Sherwood number, is presented, the impact of the emerging flow parameters on the velocity, temperature, and concentration profiles are graphically presented and discussed. The findings indicate that a greater degree of thermophoresis parameter lowers the friction factor and increases the rate of heat transfer. Additionally, for larger value of Brownian motion parameter, the thicknesses of the fluid momentum, temperature, and concentration boundary layers decrease. The drag force on the stretched cylinder is reduced by the Williamson nanofluid, and the influence of thermophoresis can limit the momentum, temperature, and concentration boundary layer properties.

KEYWORDS; Double Diffusive, Homotopy Perturbation Method, magnetohydrodynamics, Nanofluid, Stretching cylinder, Williamson

Date of Submission: 14-01-2025

Date of acceptance: 27-01-2025

I. INTRODUCTION

Any natural media that tends to continually deform under the influence of shear stress is considered fluid. Common examples include air, water, and gasses. It is impossible to overstate the significance of fluids in our existence; without them and the behaviours they exhibit, life as we know it would not exist. In actuality, fluids have a big impact on our health. Because of their extensive use in the physical and natural sciences such as the biological sciences, oceanography, geophysics, atmospheric sciences, and many more fluids are a part of our leisure systems, entertainment, and transit networks. The environmental dispersal of wastewater, rivers and lakes, pipes (crude oil extraction and drainage systems), air conditioning and heating, and waste storage (sewage transport and disposal) are all examples of industrial operations that depend on fluids.

Additionally, depending on their fluid flow characteristics, fluids are generally divided into two different groups: Newtonian and non-Newtonian fluids. Newton's law of viscosity, which states that the rate of shear stress is directly proportional to the velocity gradient that is, that the viscosity is independent of the rate of deformation is obeyed by Newtonian fluids, so named because of the linear relationship between their rate of deformation and the shear stress. Newtonian fluids, such as water, urine, and sugar solutions, have been modelled using the Navier-Stoke equation. Navier-Stokes is unable to model or capture the behaviour of non-Newtonian fluids, which are defined as fluids that do not follow Newton's law of viscosity. Shampoos, tomato pastes, toothpaste, honey, liquid plastics, cake butter, cosmetics, and gels are examples of non-Newtonian fluids, in which the relationship between shear stress and deformation rate is nonlinear. Since no single constitutive model can adequately describe the properties of non-Newtonian fluids, a variety of models are available in the literature. Viscoelastic fluid, micropolar fluid, Casson fluid, Ostwald-de Wade power-law fluid, Eyring-Powell,

Jeffery fluid, Sisko fluid, couple-stress fluid, Giesekus, tangent hyperbolic fluid, Maxwell, power-law, and Williamson fluid models are among them.

Researchers have recently focused a lot of attention on non-Newtonian fluids due to their wide range of industrial, biomechanical, engineering, and manufacturing applications, including the refinement of petroleum products, [1], the body's blood flow, sewage transportation, etc. Because of its complexity and diversity, working with non-Newtonian fluid flows presents problems for mathematicians and simulation engineers. These fluids have the characteristic that the rate of deformation and stress do not correlate linearly. These fluids include, for example, pulps, molten polymers, and some naturally occurring fluids like animal blood. A fluid is considered non-Newtonian if its viscosity changes as it moves. The viscosity of non-Newtonian fluids varies with the shear rate.

Because Newtonian fluids have limited applications, there has been interest in studying non-Newtonian fluids. Non-Newtonian fluids include things like starch, lubricating sprays, honey, and ketchup. [2], Since the well-established Navier-Stokes equations are unable to explain the rheological characteristics of non-Newtonian fluids, a variety of models have been used to describe these fluids' characteristics to overcome this constraint. This group of models includes, among others, the Ellis, Carreau, Cross, Casson, and power law models. A particular non-Newtonian model called the Williamson model was created to describe the flow of pseudoplastic materials., [3],

One of the most significant non-Newtonian fluids is the Williamson fluid, which has characteristics that are very similar to those of polymeric solutions and is characterized by a decrease in viscosity with an increase in the rate of shear stress. According to a different explanation, the effective viscosity in the Williamson fluid model should decrease endlessly as the shear rate increases. This is equivalent to having zero viscosity as the shear rate approaches infinity and infinite viscosity at stationary, [2]. Williamson investigated the flow properties of pseudo-plastic materials and created a model to explain the flow of pseudo-plastic fluids, which he later verified through experimental findings. This model is called Williamson's equation. [4],

The behaviour of Williamson fluid under convective boundary conditions on both fixed and moving surfaces was examined by [5], Khan and Khan (2014) used a Homotopy analysis method to numerically solve a non-Newtonian Williamson boundary layer flow [6], .

The growing need for more advanced heat transfer technologies cannot be satisfied by conventional heat transfer fluids with low thermal conductivity, such as water and oil. Small solid nanoparticles are added to these common fluids to increase their heat conductivity to address this problem. Thus, nanofluids are fluids created by incorporating small amounts of particles as small as nanometers into ordinary liquids. The first person to study and enhance fluids' thermal conductivity was Choi in 1995, [1]. In medical applications, such as the use of gold nanoparticles to cure cancer and the creation of microscopic agents intended to target and eliminate malignant tumours, nanofluids are crucial, [7]. Research on nanofluids has gained attention in recent years. [8] suggested a nonhomogeneous nanofluid model that incorporates the effects of thermophoresis and Brownian diffusion by considering the relative velocity of nanoparticles and fluids. Tiwari-Das updated Buongiorno's model in 2009 and developed a framework for analyzing how nanofluids behave about the volume percentage of nanoparticles. It was expected that the nanoparticles would be uniformly distributed throughout the base fluid, [9].

Heat and mass transfer play important roles in fluid dynamics. When a fluid passes across a surface, mass and heat are transferred. Frictional forces are another source of heat generation in addition to external heat sources. Heat and mass transfer have many uses in air conditioning systems, refrigerator compressors, car engines, and other thermodynamic devices, [10]. In recent years, there has been a surge in interest in studying fluid flow across a stretching sheet because of its crucial importance in industries including metal spinning, plastic films, polymer extrusion, and metallurgical processes, [3]

Because of its many uses in the extrusion process, metal extraction, annealing, copper wire thinning, and the pipe industry, the heat and mass transfer in the boundary layer flow of non-Newtonian fluids over a stretching cylinder is important to scientists, engineers, and researchers, [11]. The study of fluids with electromagnetic conductivity, such as plasma, metallic, and saline fluids, is known as electromagnetic fluid dynamics, or magnetohydrodynamic fluid, [7]. By combining fluid mechanics and electromagnetism, magnetohydrodynamics (MHD) describes how an electrically conducting fluid interacts with a magnetic field. Alfvén carried out the first investigation on this topic in 1942. [12]

MHD water-based nanofluids under convective boundary conditions were studied by [13]. Endoscopy, cancer tumour treatment, blood flow, cell separation, centrifugal turbines, and tissue temperature control are among the fields that use magnetohydrodynamics [2]. The investigation of magnetohydrodynamic (MHD) heat and mass transfer flow has gained considerable significance in engineering technology industries over the past few decades. The influence of magnetic fields with constant or varying field strengths, for numerous natural and artificial flows whether they are diagonally placed to the direction of flow or inclined at an angle cannot be over-emphasized. This is because magnetic fields are important in producing electricity in thermal power

stations, heating, magnetic stirring, levitation of molten metal and confinement of some high-temperature electrically conducting pollutants and nuclear wastes in industrial processes, [14]

Double diffusion is a fascinating and challenging phenomenon in fluid dynamics. It is described as a fluid of mass and heat due to co-diffusion, which produces intricate patterns and behaviours. It is difficult to comprehend double diffusion since so many diverse factors interact. Researchers employ a variety of techniques, such as numerical simulations, laboratory testing, and mathematical models, to examine this phenomenon and its effects in diverse circumstances. Using the Keller-Box technique, the boundary layer flow of nanofluids in an unstable double-diffusive variable convection flow across an erect area close to an inertia point movement was investigated, [15]. The impact of convective boundary constraints and nonlinear thermal radiation on the mass and heat transfer of an allowed convective Casson fluid inertia point stream across a moving vertical plate was investigated [16]. How the radiative and reactive Prandtl nanofluid cross-diffusion is affected by a stretched convectively heated surface was investigated [17] and quantitative studies on the impact of double-diffusive nonlinear free convective flow of liquids flowing over various surfaces was conducted [18]. In a new W-shaped porous cavity, the mixed thermo-bioconvection of magnetically sensitive fluid containing copper nanoparticles and oxytactic bacteria was investigated [19]. The governing partial differential equation of Williamson fluid is converted into an ordinary differential equation using similarity transformations along with the boundary layer approach, which is then solved analytically by applying the Homotopy Perturbation Method. The effect of different parameters on velocity, temperature and concentration profiles are thoroughly examined through graphs and tables.

Williamson fluids and nanofluids in the context of over-stretching cylinders and plates have not received much attention from scientists and engineering authors. The double-diffusive flow of a dusty Williamson MHD nanofluid over a permeable stretched cylinder in a porous media, however, has not been studied, according to the review of prior research. The difficulties presented by nonlinear coupled equations have been recognized by researchers, who have been unable to overcome this problem analytically (HPM).

The Previous Methods in the Past Studies for Boundary Layer Flow Problem

Based on the importance and various applications of Williamson fluid, various researchers have presented different studies in literature in order to describe the flow pattern and behaviour of the non-Newtonian fluid under various factors and conditions.

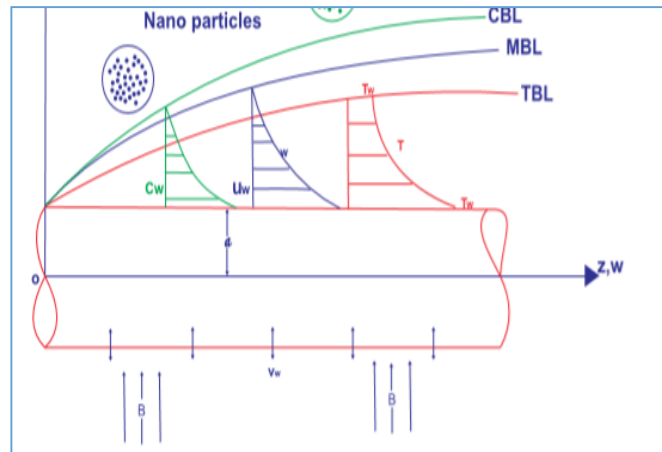
Table 1: Methods used by previous authors in literature

Authors	TITLES	METHOD
Salahuddin et. al. (2024)	Adaptation of Nanofluids with MHD Williamson fluid to enhance the thermal and solutal analysis with viscous dissipation. A numerical study	Adam-Bashforth Predictor and corrector method and Runge-Kutta- 4 scheme and secant method
Muzara & Shateyi (2023)	MHD Williamson Nanofluid Flow over an Exponentially Stretching Surface with a Chemical Reaction and Thermal Radiation.	Spectra quasi-linearization method
Ullah et. al. (2023)	Electro-magnetic radiative flowing of Williamson-dusty nanofluid along elongating sheet, Nanotechnology application	The Runge-Kutta Fehlberg approach (RKFA)
Amjad et.al. (2022)	Numerical Solution of Magnetized Williamson Nanofluid Flow over an Exponentially Stretching Permeable Surface with temperature dependent viscosity and thermal conductivity	BVP4C (boundary value problem solver
Umehaiah et. al. (2022)	Dusty Nanoliquid Flow through a Stretching Cylinder in a Porous Medium with the Influence of the Melting Effect	Runge-Kutta with shooting method
Arifin et.al. (2021):	Boundary Layer Flow of Dusty Williamson Fluid with Variable Viscosity Effect Over a Stretching Sheet.	Keller-box method.
Varun Kumar et. al. (2021)	Two-phase flow of dusty fluid with suspended hybrid nanoparticles over a stretching cylinder with modified Fourier heat flux	Runge-Kutta-Fehlberg fourth fifth order inclusive of shooting approach.

II. MATERIALS AND METHODS

Figure 1 depicts the schematic diagram illustrating the two-dimensional Williamson MHD nanofluid on a stretching cylinder through a porous medium. Temperature, velocity and concentration on the surface are

denoted by $T_w U_w$ and C respectively whilst the ambient fluid temperature, velocity and concentration are denoted by $T_\infty U_\infty$ and C_∞ respectively. Furthermore, w and u are the velocity components in the direction of z and r axis respectively.



The following assumptions are made:

- I. The axis is perpendicular to the axis measured along the cylinder's axis.
- II. External magnetic polarization and electric fields do not interfere.
- III. It is believed that a homogenous magnetic field of strength is applied parallel to the $-z$ -axis and normal to the surface.
- IV. In comparison to the applied magnetic field, the induced magnetic field is relatively small since the magnetic Reynolds number is minimal.
- V. The permeability coefficient of a porous media remains constant as the viscosity coefficient and heat conductivity of thermofluids vary.
- VI. There is no slippage and the fluid and porous medium are in constant thermal balance

2.1 Governing equations of the problem:

Continuity Equation,

$$\frac{\partial(ru)}{\partial r} + \frac{\partial(rw)}{\partial z} = 0 \tag{1}$$

Momentum Equation

$$u \frac{\partial w}{\partial r} + w \frac{\partial w}{\partial z} = \nu_{nf} \left(\frac{1}{r} \frac{\partial w}{\partial r} + \frac{\partial^2 w}{\partial r^2} \right) + \nu_{nf} \left[\frac{\Gamma}{\sqrt{2}} \left(\frac{\partial T}{\partial r} \right)^2 + \sqrt{2} \frac{\partial w}{\partial r} \frac{\partial^2}{\partial r^2} \right] + \frac{KN}{\rho_{nf}} (w_p - w) - \left(\frac{\sigma B_0^2}{\rho_{nf}} + \frac{\nu_{nf}}{k_p} \right) w \tag{2}$$

Energy Equation,

$$w \frac{\partial T}{\partial z} + u \frac{\partial T}{\partial r} = \frac{k}{\rho c_p} \left(\frac{1}{r} \frac{\partial T}{\partial r} + \frac{\partial^2 T}{\partial r^2} \right) + \tau \left\{ D_B \frac{\partial C}{\partial r} \frac{\partial T}{\partial r} + \frac{D_T}{T_\infty} \left(\frac{\partial T}{\partial r} \right)^2 \right\} + \frac{Q_0}{(\rho c_p)} (T - T_\infty) \tag{3}$$

Concentration Equation

$$w \frac{\partial C}{\partial z} + u \frac{\partial C}{\partial r} = D_B \frac{\partial^2 C}{\partial r^2} + \frac{D_T}{T_\infty} \left(\frac{\partial^2 T}{\partial r^2} \right) \tag{4}$$

where (w, u) stand for the z -directional velocities of the nanofluid phase and the r -directional velocities of the dust phase, respectively. The symbols $\nu, \rho, N, m,$ and K stand for the variables kinematic viscosity, fluid density, number density of the particle phase, dust particle mass, Stoke's resistance (drag coefficient), and permeability of the porous media, respectively. Additionally, the fluid's density is represented by ρ , and the thermal diffusivity by α . Thermophoretic diffusion coefficient is indicated by D_T while the Brownian diffusion coefficient is shown by D_B .

$$w = U_w, \quad u = 0, \quad T = T_w = T_\infty, \quad C = C_w = C_\infty \text{ at } r = a$$

$$w \rightarrow 0, \quad u = 0, \quad T \rightarrow T_\infty, \quad T_p \rightarrow T_\infty, \quad C \rightarrow C_\infty \text{ as } r \rightarrow \infty$$

A stream function (ψ) that satisfies the continuity equation is shown, denoted as ψ .

$$u = -\frac{1}{r} \frac{\partial \psi}{\partial r} \text{ and } w = -\frac{1}{r} \frac{\partial \psi}{\partial z}$$

2.2 Non-dimensional form of the Governing Equations

In order to obtain the dimensionless Continuity, Momentum, Energy and Concentration equations respectively, the following non- dimensionless variables was introduced as stated by anjunatha,(2017)

$$\eta = \frac{r^2 - a^2}{2a} \sqrt{\frac{u_w}{vz}}, \quad \psi = a \sqrt{\nu_f u_w z} f(\eta), \quad \theta = \frac{T - T_\infty}{T_w - T_\infty}, \quad w = u_w(z) f'(\eta), \quad u = -\frac{a}{r} \sqrt{\frac{\nu_f u_w}{z}} f(\eta), \tag{5}$$

The variables η , f , and θ represent the dimensionless transverse distance, dimensionless stream function, and dimensionless temperature of the fluid, respectively. The kinematic viscosity $\nu = \frac{\mu_\infty}{\rho}$. After applying above

transformations to the governing equations we obtain the following dimensionless form of the three equations

$$\phi_1 \{ (1 + 2\gamma\eta) f''' + 2\gamma f f'' \} + \phi_1 We (1 + 2\gamma\eta)^{\frac{1}{2}} \left[\gamma f'^2 + 2 \{ \gamma f f'' + (1 + 2\gamma\eta) f''' \} \right] + \phi_2 (ff'' - f'^2) - \beta\beta_c (f' - F') - (\phi_3 Ha + \phi_1 Da) f' = 0 \tag{6}$$

$$\frac{\phi_1 \phi_A}{Pr} \{ (1 + 2\gamma\eta) \theta'' + 2\gamma \theta' \} + \phi_1 \phi_3 (\theta' f - 2\theta f') + \phi_1 \phi_2 Ha \cdot Ec (f')^2 + \frac{\phi_2 \phi_A}{Pr} (A f' + B \theta) + \phi_1 \beta_T \beta (\theta_p - \theta) = 0 \tag{7}$$

$$\phi'' + Sc f \phi' + \left(\frac{N_T}{N_B} \right) \theta'' + \beta_c \phi' = 0 \tag{8}$$

And the corresponding dimensionless BCs for the prescribed surface temperature (PST)

$$f(\eta) = f_w, \quad f'(\eta) = 1, \quad \theta(\eta) = 1 \quad \phi = 1 \quad \text{at } \eta = 0, \tag{9}$$

$$f'(\eta) = 0, \quad F'(\eta) = 0, \quad F(\eta) = f(\eta) \quad \theta(\eta) = 0, \quad \text{as } \eta \rightarrow \infty$$

The dimensionless equations contain the following emergent parameters:

$$Pr = \frac{\mu_c p}{k}, \text{ is Prandtl number. } Ha = \frac{\sigma_f B_0 w}{\rho_f U_f} \text{ is Hartmann number,}$$

$$\gamma = \frac{1}{a} \sqrt{\frac{\nu_f z}{u_w}} \text{ is Curvature parameter, } K = \frac{z}{\tau u_w}, \text{ is porosity parameter, } Ec = \frac{u_w z}{Ac_p} \text{ is Eckert,}$$

$$\lambda = \Gamma \sqrt{\frac{2u_w}{\nu_n f z}} \text{ is the Weissenberg parameter, } N_t = \frac{\tau D_T}{\nu T_\infty} (T_w - T_\infty) \text{ is the thermophoresis parameter,}$$

$$N_b = \frac{\tau D_B}{\nu} (C_w - C_\infty) \text{ Brownian motion, } Sc = \frac{\nu}{D_B} \rightarrow \text{Schmidt number} \tag{10}$$

2.2 Parameters of physical and engineering interest for the problem

In addition to determining the velocity, temperature and concentration distributions, it is often desirable to compute other physically important quantities (such as shear stress, drag, heat transfer rate, and concentration) associated with the free convection flow and heat transfer problem. Consequently, three parameters, The Physical quantities of engineering interest are skin friction coefficient, (C_f), Nusselt numbers (Nu) and Sherwood number (Sh) which physically indicate the wall shear stress, rate of heat transfer and rate of mass transfer, respectively. They are defined respectively as follows:

$$\left. \begin{aligned} C_{fz} &= \frac{\tau_w}{\rho_n f U_w} , \\ Nu_z &= \frac{q_w}{k_f (T_w - T_\infty)} \\ Sh_z &= \frac{m_w}{Dm_\infty (C_w - C_\infty)} \end{aligned} \right\} \tag{11}$$

τ_w is the shearing stress, q_w is the heat flux and m_w is the mass flux at the surface and Dm_w is the diffusion constant respectively and defined as

$$\begin{aligned} \tau_w &= \mu_{nf} \left[\frac{\partial u}{\partial r} + \frac{r}{\sqrt{2}} \left(\frac{\partial u}{\partial r} \right)^2 \right]_{r=a} \\ q_w &= -k_{nf} \frac{\partial T}{\partial r} \Big|_{r=a} = -k_{nf} \frac{\Delta T r}{a} \sqrt{\frac{U_w}{\nu_{fz}}} \theta'(\eta) \Big|_{r=a} \\ m_w &= -Dm \frac{\partial C}{\partial r} \Big|_{r=a} \end{aligned} \tag{12}$$

Using the dimensionless variables we obtain

$$\begin{aligned} Re_z^{\frac{1}{2}} C_{fz} &= \frac{\phi_1}{\phi_2} [f''(0) + We f''^2(0)], \\ Re_z^{-\frac{1}{2}} N u_z &= (-\theta'(0)), \\ Re_z^{-\frac{1}{2}} S \square_z &= (-\phi'(0)) \end{aligned} \tag{13}$$

Local Reynold's number $Re_z = \frac{U_w z}{\nu_{nf}}$

III. METHOD OF SOLUTION

The Homotopy Perturbation Method (HPM) was used to achieve the semi-analytical solution because the reduced set of similarity equations are coupled and nonlinear, making it very difficult to obtain accurate answers. Since HPM successfully combines homotopy theory with perturbation theory, it is essential in this situation. The fundamental idea is that a complex problem is continuously broken down into a simpler, easier one in order to arrive at an approximation or semi-analytic solution.

3.1 Analysis of the Nonlinear Model

In the same way, the governing equation of the model can be converted to dimensionless forms by employing the similarity transformation defined in (equation 5)

Consider the following system of nonlinear ordinary differential equations: there are three equations in total. The equations governing the fluid phase are those that describe the velocity, energy and concentration equations respectively.

Velocity Equation

$$\phi_1 \{ (1 + 2\gamma\eta) f''''(\eta) + 2\gamma f''^3(\eta) \} + \phi_1 \lambda (1 + 2\gamma\eta)^{\frac{1}{2}} [\gamma f''^2 + 2\{ \gamma f'' + (1 + 2\gamma\eta) f'''' \}] + \phi_2 (f(\eta) f''(\eta) - f'^2) - l\beta_v (f'(\eta) - F'(\eta)) - (M + K) f'(\eta) = 0 \tag{14}$$

Energy Equation

$$\begin{aligned} \frac{\phi_1 \phi_4}{Pr} \{ (1 + 2\gamma\eta) \theta'' + 2\gamma \theta'^2 \} + \phi_1 \phi_3 (\theta' f - 2\theta f') + N_b \phi' \theta' + N_t \theta'^2 + \phi_1 \phi_2 l\beta_t \theta' \\ + M \cdot l\beta_t Ec (F'(\eta) - f(\eta)) = 0 \end{aligned} \tag{15}$$

Concentration equation

$$\phi'' + Le f \phi' + \left(\frac{N_T}{N_B} \right) \theta'' = 0 \tag{16}$$

IV. Results and Discussion

4.1 Verification of results

A direct comparison with published findings from other research studies in the literature, which serve as specific cases of the current investigation, has been done in order to confirm the accuracy of the conclusions produced in this study. A summary of the Model, including the absolute relative difference, is shown in Tables 2 and 3. Section 4.2 provides a graphic representation and analysis of the effects of physical parameters on the dimensionless velocity, $f(\eta)$, temperature, $\theta(\eta)$, and concentration, $\phi(\eta)$ profiles. Additionally, In particular, the local skin friction coefficient, (wall shear stress), Nusselt number (rate of heat transfer), and the local Sherwood number (mass transfer at the permeable cylinder surface) are all examined in relation to the effects of the relevant parameters. Tables and graphs have been used to display the data. The values of $f'(0)$ are contrasted with the findings of [21], who used the Runge–Kutta–Fehlberg fourth-fifth order approach for their solution, by using different values for the effective Hartman's number and setting all other parameters to zero in Table 2. The

comparisons show that the current study and the body of existing literature are highly aligned. This validates the current findings and the correctness of the analytical method used by confirming that the HPM used in this investigation is accurate and dependable. As a result, we claim that our findings are highly accurate for the investigation of this boundary layer flow problem

Pr	$f''(0)$ [21]	Present work (HPM) $f''(0)$	$-\theta'(0)$ [22]	Present work (HPM) $-\theta'(0)$
0.72	-0.3645	0.3645	-1.08850	-1.08850
1.0	-1.41425	-1.41425	-1.3333	-1.3333
3.0	-160873	-160873	-1.4287	-1.4287
5.0	-2.44948	-2.44948	-1.5295	-1.5295
10	-3.31662	-3.31662	-2.2960	-2.2960

Table 2 Comparison of the present results for the dimensionless temperature gradient $-\theta'(0)$ and velocity $f''(0)$ with previous published work of Kumar et al and Giresha et. al. respectively

M	λ	Pr	N_T	N_B	C_f	Nu	Sh
0.1 0.5 1.0	0.35	0.5	0.2	0.2 -2	1.00362248 1.0052563 1.10235693	0.34332325 0.427321112 0.462531215	0.312335620 0.402895613 0.428746329
		0.75 1.5		-2	1.13523321672 1.10599847326 1.12012252439	0.489221753 0.46823113 0.48623893	0.621392656 0.523694821 0.452368903
	0.2 0.5		0.5 0.8 1.2		1.1528946113 1.2058912333 1.2257890369	0.553269423 0.578421369 0.548213694	0.523216156 0.625369513 0.652314789
		0.5		0.5 0.8 1.2	1.1325648974 1.2035644894 1.2521564891	0.578421369 0.548213694 0.632598794	0.625369513 0.652314789 0.72532123

Table 1: Effects of Ha, λ, N_T , and N_B on local Skin friction coefficient C_f , Nusselt number (Nu) and Sherwood number (Sh)

The Effects of Physical Parameters on the dimensionless Velocity Profile

Table 3, shows that the drag forces are better minimized when using the Williamson nanofluid. This is a very important finding that has implications for several engineering procedures. Additionally, for the Williamson nanofluid scenario, the rate at which species mass is moved away from the cylinder surface is accelerated for all of these characteristics taken into consideration. It has been found that when the (Wesseinberg) parameters fall, the skin-friction coefficient lowers; nevertheless, when the magnetic parameter increases, it increases. Table 3 further shows that a decrease in the Nusselt number results from a decrease in the thickness of the thermal boundary layer when the Wesseinberg parameter is increased. A stretched surface will cause flow if the skin friction coefficient, or C_f , is physically negative. This indicates that the surface is exerting a drag force on the fluid. Additionally, it was noted that the Sherwood number dramatically drops when the porosity parameter, K , increases. Also Table 3 shows the Skin-friction coefficient appreciates in terms of numbers variations in terms of the engineering parameters such as, M , Pr , λ , Nt , and Nb . It can be seen from the above chart that the Skinfriction coefficient is increasing by means of rising values of Nt in addition to while it is decreasing raising the value of M , Nb , and Pr . The numerical values of convective heat transfer coefficient when it comes to Nu are exhibited in Table 3 for various values of Nt , Nb and Pr . The rate of heat transfer coefficient is gradually rising with increasing values of Nt and Nb while the reverse effect is observed in rising the value of Pr . The impact of Brownian motion Nb and thermophoresis Nt on coefficient of mass transfer rate or Sherwood number.

4.2 Graphical representation

Figure 2 shows the effects of the stretching parameter. In Figure 1(a) increase in the stretching parameter ($\lambda = 2$) increases the velocity of nanofluid. This is caused by a stretch which reduces the viscous effect on the flow. As a result momentum boundary layer thickness is reduced with increasing stretching parameters hence increased nanofluid velocity. Figure 3 depicts the effects of Weissenberg parameter (We), λ , on the fluid and dust phases velocity distribution. Increasing the λ parameter reduces the magnitude of the fluid velocity for shear thinning fluid while it rises for the shear thickening fluid. The ratio of relaxation time to retardation time is represented by the Wesseinberg parameter, λ . As the values of λ , rise, the relaxation time of fluid molecules similarly increases. This leads to an augmentation in dynamic viscosity, which in turn causes obstructions to the movement of the fluid, thus leading to a reduction in fluid flow. The change in the fluid temperature plays an important role in the fluid's behaviour in addition to its effect also on the particles inside the fluid. Fig-4 shows the variation of the non-dimensional temperature profile for various values of Prandtl number, Pr . The Prandtl number can be viewed as the ratio of momentum to thermal boundary layers. Physically, a high Prandtl number means a small thermal boundary layer which increases the gradient of the temperature. It is observed that an increase in the value of Pr leads to a decrease in temperature profiles. As the Prandtl number, Pr , rises, the temperature and thermal boundary layer thickness rapidly fall. A higher Prandtl number results in a higher fluid viscosity, which lowers the temperature profiles. This is also in line with the observation that as the Prandtl number Pr increases, the thermal boundary thickness decreases.

The Williamson model describes the rheological behaviour of a non-Newtonian fluid, also known as a Williamson nanofluid, and is influenced by both Brownian and thermophoresis variation. The application of thermophoresis and Brownian motion is important for nanofluids. The thermophoresis parameter Nt is essential for examining the temperature distribution and nanoparticle volume fraction in nanofluids. Figure 5 and 6 illustrate the impact of the thermophoresis parameter Nt on the temperature profile and the concentration profile (nanoparticle volume fraction). Figures 5 and 6 indicate that when Nt increases, both the fluid temperature and the concentration profiles rise. An overshoot along the wall has been identified, whereas a reversal tendency is noted further from the border. Increasing Nt results in an enhancement of the thermophoresis force, which facilitates the movement from hot to cold regions, hence augmenting the magnitude of temperature profiles and the concentration profile. The thickness of the concentration (nanoparticle volume) boundary layer increases substantially with a slight increase in the thermophoresis parameter Nt . Figures 7 and 8 depict the influence of the Brownian parameter Nb on the temperature and concentration profiles, respectively. The figure indicates that the fluid's temperature rises with an increase in Nb and the concentration profiles (volume of nanoparticles) diminish with an increase in Nb . In a nanofluid system, the presence of nanoparticles induces Brownian motion, and an increase in nanoparticle concentration (Nb) influences this motion, hence altering the fluid's heat transmission characteristics. The thickness of the nanoparticle volume boundary layer diminishes as Nb increases.

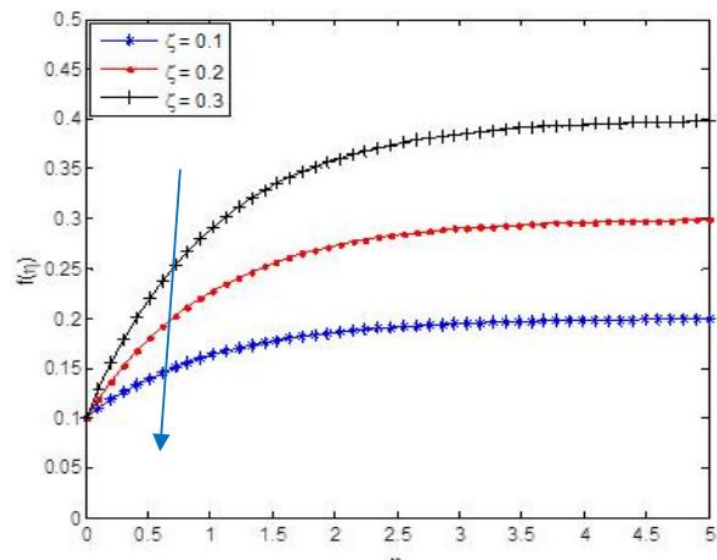


Figure 2: Effect of stretching parameter on velocity profile

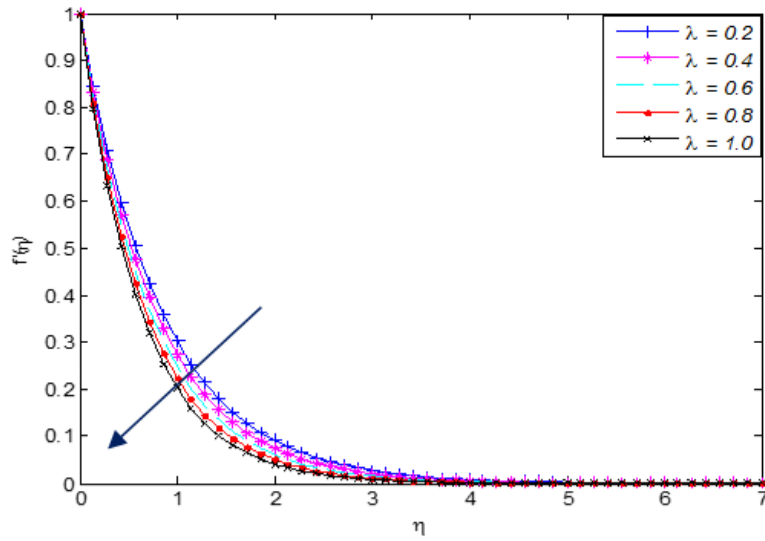


Figure 3: Effect of Wesseinberg Parameter on the velocity profile

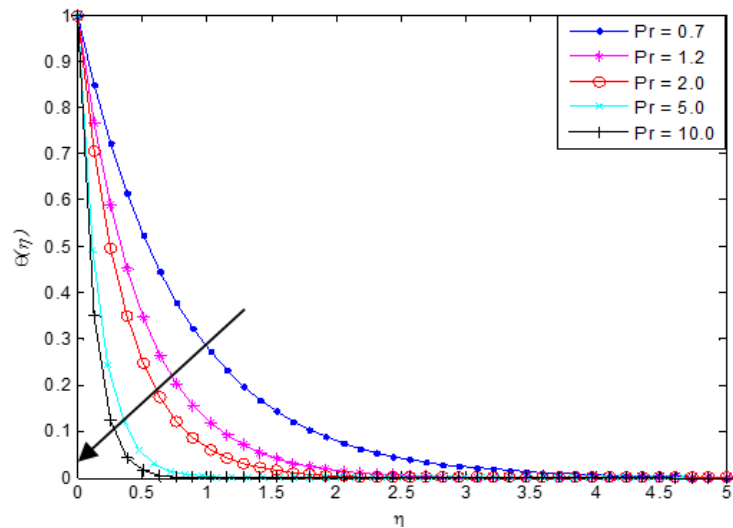


Figure 4: Effect of Prandtl number on temperature profile

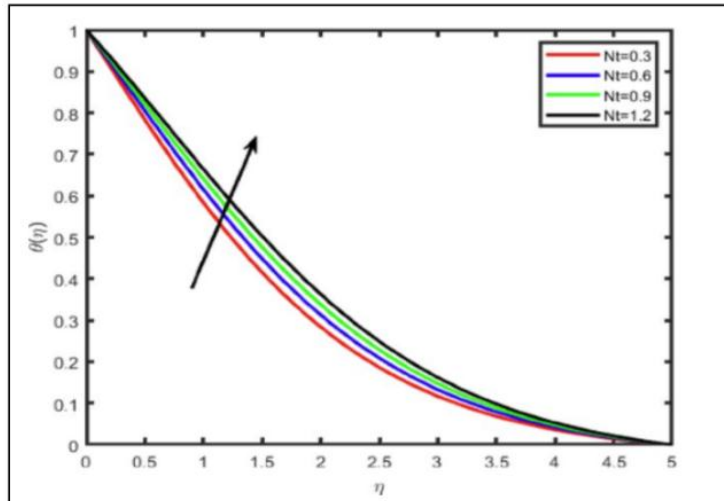


Figure 5: Effect of Thermophoresis parameter on Temperature profile.

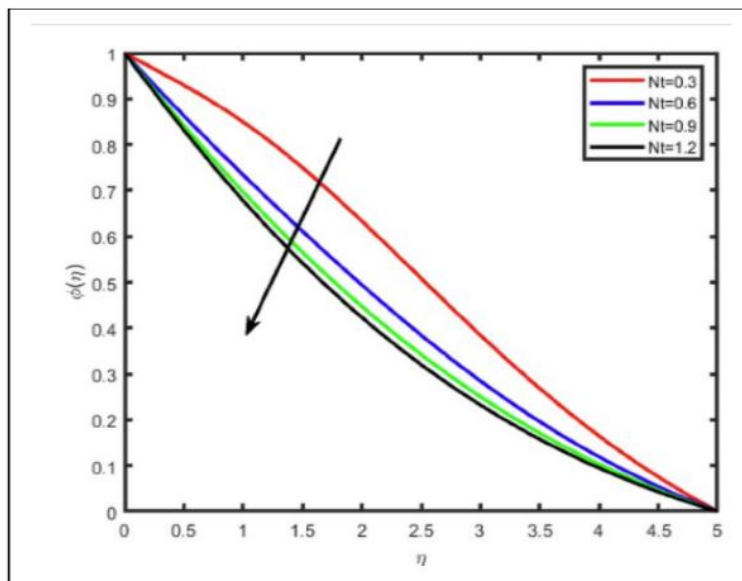


Figure 6: Effect of Thermophoresis parameter on concentration profile.

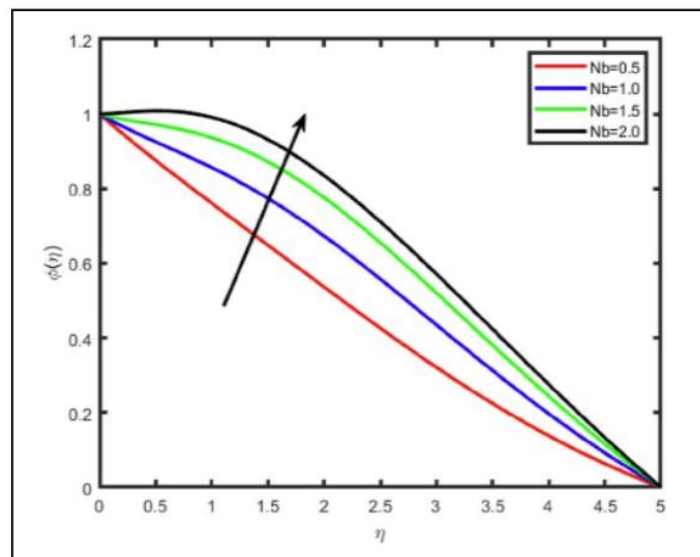


Figure 7: Effect of Brownian motion on concentration profile

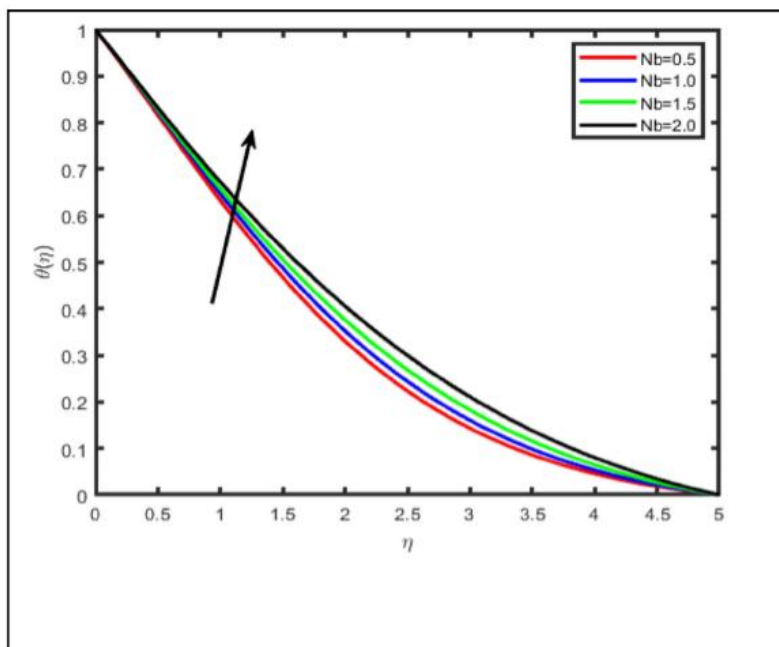


Figure 8 Effect of Brownian motion on temperature profile

V. CONCLUSION AND CONTRIBUTIONS TO KNOWLEDGE

5.1 Conclusion

In the present study, the governing equations of double diffusive MHD boundary layer flow of Williamsonnanofluids over a nonlinear stretching cylinder is considered. semianalytical solutions are obtained by means of Matlab's Homotopy Perturbation Method (HPM). The study includes a graphic representation and analysis of the skin friction coefficient, Nusselt number, Sherwood number, concentration, temperature, and velocity profiles, along with the influence of other regulating parameters. The primary findings of this study were as follows:

- Increasing values of stretching parameter result in a reduction in the velocity profile as well as the momentum boundary layer thickness.
- Wesseinberg parameter decreases the rate of flow and the boundary layer thickness in the fluid
- As the Prandtl number, Pr, increases, the temperature profiles of the fluid phase grow flatter and reduces. A fluid with a higher Prandtl number has a lower thermal conductivity, which implies less conduction.
- The temperature profiles and the nanoparticle volume fraction increases with the increase of Nt. The effect of Nb, leads to enhance the temperature profiles and reduces concentration profil

5.2 Contributions to Knowledge

Researchers have accepted that nonlinear coupled differential equations are notoriously challenging to solve analytically, and they now prefer to use numerical methods instead.

- Thus, this study has been successful in solving the simulated problems with the use of the analytical approach (HPM).
- This thesis created a hydrothermal flow model that took into account the flow's nanoparticles.
- The coupled nanofluid hydrothermal flow model behavior was analytically solved in this work.

ACKNOWLEDGEMENTS

The authors are grateful to the authors referred in this work.

CONFLICTS OF INTEREST

The authors declare no conflict of interest

REFERENCE

- [1]. Malik, M.Y. Salahuddin, T. Hussain, A., Bilal, S. and Awais, M. (2015). Homogeneous-heterogeneous reactions in Williamson fluid model over a stretching cylinder by using Keller box method, AIP Advances 5.
- [2]. Amjad, M. Ahmed, I. Ahmed, K. Alqarni, M.S. Akbar, T. Muhammad, T. Numerical Solution of Magnetized Williamson Nanofluid Flow over an Exponentially Stretching Permeable Surface with temperature dependent viscosity and thermal conductivity, (2022): Nanomaterials, vol.12, pp. 3661.

- [3]. Muzara, H. Shateyi, S.(2023): Magnetohydrodynamics Williamson Nanofluid Flow over an Exponentially Stretching Surface with a Chemical Reaction and Thermal Radiation. Mathematics, 11, 2740.
- [4]. Williamson, R.V. (1929): The flow of pseudoplastic materials, Industrial and Engineering Chemistry: vol. 21, no. 11, pp. 1108–1111.
- [5]. Ramesh, G. K. Gireesha, B. J. and. Bagewadi C. S, (2012): Heat transfer in MHD dusty boundary layer flow over an inclined stretching sheet with non-uniform heat source/sink, Advances in Mathematical Physics, 2012 (657805) , 1-13.
- [6]. Khan, N.A. and Khan, H. (2014). A boundary layer flows of non-Newtonian Williamson fluid. Nonlinear Engineering,3,107-115.
- [7]. Bouslimi, J., Omri, M., Mohamed, R. A. Mahmoud, K. H., Abo-Dahab, S. M. and Soliman, M. S.(2021). MHD Williamson nanofluid flow over a stretching sheet through a porous medium under effects of joule heating, nonlinear thermal radiation, heat generation/absorption, and chemical reaction. Advances in Mathematical Physics, 2021.,
- [8]. Buongiorno, J. (2006): Convective Transport in Nanofluids. ASME Journal of Heat Transfer, 128(3), 240–250.
- [9]. Tiwari, R.K. and Das, M.K. (2007). Heat transfer augmentation in a two-sided lid-driven differentially heated square cavity utilizing nanofluids. International Journal of Heat Mass Transfer,50.
- [10]. Nazir, I., Muhammad, K., Ahmed, Z., Hamed, A. and Madeeha, G.(2022): A study of heat and mass transfer of Non-Newtonian fluid with surface chemical reaction, Journal of the Indian Chemical Society, 99(5).
- [11]. Ibrahim, W. and Negera, M. 2020. The Investigation of MHD Williamson Nanofluid over Stretching Cylinder with the Effect of Activation Energy. Advance in Mathematical Physics,9523630,1-16
- [12]. Alfvén, H. Existence of Electromagnetic-Hydrodynamic Waves. 1942: Nature 150, no. 3805, pp.405–406.
- [13]. Wakif A., Boulahia Z., Amine A., Animasaun I. L., Afridi M. I., Qasim M., Sehaqui R. (2019): Magneto-convection of alumina - water nanofluid within thin horizontal layers using the revised generalized Buongiorno's model. Frontiers in Heat and Mass Transfer,12,3.
- [14]. Davidson, P.A. (2001): An Introduction to Magnetohydrodynamics. Cambridge University Press.UK:
- [15]. Islam, A., Mahmood, Z. & Khan, U. (2023): Double-diffusive stagnation point flow over a vertical surface with thermal radiation: Assisting and opposing flows. Sci. Progr.106, 10.1177
- [16]. Nandeppanavar, M. M., Kemparaju, M. C. & Raveendra, N.(2021): Effect of non-linear thermal radiation on the stagnation point flow of double diffusive free convection due to moving vertical plate. J. Eng. Design Technol.21(1), 150–166.
- [17]. Patil, A. B., Patil, V. S., Humane, P. P., Shamshuddin, M. D. & Jadhav, M. A. (2021): Double diffusive time-dependent MHD Prandtl nanofluid flow due to linear stretching sheet with convective boundary conditions. Int. J. Modell. Simulat.43(1), 34–48.
- [18]. Mandal, D. K., Biswas, N., Manna, N. K., Gorla, R. S. R. & Chamkha, A. J. (2023): Hybrid nanofluid magnetohydrodynamic mixed convection in a novel W-shaped porous system. Int. J. Num. Methods Heat Fluid Flow33, 510–544
- [19]. Biswas, N., Mandal, D. K., Manna, N. K. & Benim, A. C. Magneto-hydrothermal triple-convection in a W-shaped porous cavity containing oxytactic bacteria. Sci. Rep.12, 18053 (2022)
- [20]. Chatterjee, D., Biswas, N., Manna, N. K. & Sarkar, S. (2023): Effect of discrete heating-cooling on magneto-thermal-hybrid nanofluidic convection in cylindrical system. Int. J. Mech. Sci.238, 107852
- [21]. Adekanmbi-Akinseye O.A., Fenuga O.J., Isede H.A., Sobamowo M.G. (2024): Flow and heat transfer of a dusty Williamson MHD Nanofluid flow over permeable cylinder in a porous medium, OJFD, Vol 14 No 2.
- [22]. Gireesha, B.J., Mahanthesh, B., Manjunatha, P.T., Gorla, R.S.(2015). Numerical solution for hydromagnetic boundary layer flow and heat transfer past a stretching surface embedded in non-Darcy porous medium with fluid-particle suspension. Journal of the Nigerian Mathematical Society, 34, 267–285
- [23]. Kumar, K. G., Rudraswamy, N.G., Gireesha, B.J. and Manjunatha, S.(2017). Non linear thermal radiation effect on Williamson fluid with particle-liquid suspension past a stretching surface, Results in Physics, 7, 3196-3202.

NOMENCLATURE

u, w	Fluid-phase velocity components
μ	Dynamic viscosity
ν	Kinematic viscosity
q_w	Thermal flux at the fluid temperature surface
T_w	Wall temperature
T	Temperature of the Nano fluid
T_∞	Ambient Temperature
a	Radius of the cylinder
D_m	Mass diffusivity
I	Identity tensors
M	Magnetic fluid parameter
q_w	Thermal flux
λ	Wesseinnberg number
V_w	Velocity at the wall
β	Fluid particle interaction parameter
θ	Dimensionless temperature
S	Heat source/sink parameter
B_0	Magnetic field strength
C_{fz}	Skin-friction coefficient
Nu_z	local Nusselt number
Re_z	Reynolds number
f, f'	Dimensionless velocities of fluid phase
F, F'	Dimensionless velocities of dust phase
D_B	Brownian diffusion coefficient [m ² s ⁻¹]

D_T Thermophoresis diffusion coefficient [$m^2 s^{-1}$]
 τ_V The relaxation time of dust particles
 M Magnetic parameter
 Pr Prandtl number
 N_f Nanofluid
 Ec Eckert number
 α Thermal diffusivity
 Γ Positive time constant
 K Porosity parameter
 f_w Volumetric fraction parameter
 ψ Stream function
 γ Curvature parameter
 ζ Stretching parameter